

THE RADIOBRIGHTNESS OF FREEZING TERRAIN

B. Zuerndorfer, A. W. England, and G. H. Wakefield

Radiation Laboratory
 Department of Electrical Engineering and Computer Science
 The University of Michigan
 Ann Arbor, MI 48109

ABSTRACT

The combination of a low 37 GHz radiobrightness and a negative 10.7, 18, and 37 GHz spectral gradient appears to be an effective discriminant for classifying frozen ground. The spatial resolution of lower frequency, satellite borne, microwave radiometers is typically relatively coarse, e.g., 100 Km for the 10.7 GHz channel of SMMR. With certain restrictions, scale-space theory can be used to map freeze/thaw boundaries that are identified at the poorest resolution of a multiband image to images having the highest resolution. That is, the process permits classification at lower resolution, but boundary location at higher resolution.

INTRODUCTION

Soil moisture contributes to the energy exchange between the air and the ground through latent heats of fusion and vaporization. The processes of thawing frozen ground or of evaporating soil moisture cause soil thermal inertias to appear anomalously high. Microscale and mesoscale climate models benefit from estimates of the amount and state of soil moisture as part of their boundary conditions.

There is a large body of literature about deriving soil moisture from radiobrightness [e.g. Burke et. al., 1979; Wang et. al., 1982; Blanchard and Chang, 1983; Schmugge, 1983; Jackson et. al., 1984; Camillo and Schmugge, 1984; Schmugge et. al., 1986; and Grody, 1988]. In addition, there is strong evidence that moisture state can also be inferred from radiobrightness. Using data from the Nimbus-7 Scanning Multichannel Microwave Radiometer (SMMR) for a test area that included North Dakota and parts of the surrounding states and southern Canada, Zuerndorfer et. al. [1989] showed that a combination of low 37 GHz radiobrightness and a negative spectral gradient of radiobrightness offers an encouraging Freeze Indicator, or discriminant, for classifying frozen terrain.

A fundamental problem with the Freeze Indicator algorithm developed by Zuerndorfer et. al. [1989] is that radiobrightness measurements from different frequency channels having different spatial resolutions are required to estimate a spectral gradient. To make each radiobrightness value refer to a common area on the ground, data from each channel is compensated to a common, coarse resolution (i.e., the resolution of the lowest frequency SMMR channel that contributes to the gradient estimate). As a result, identified freeze/thaw boundaries are localized only to the accuracy of the resolution of the lowest frequency channel that was used.

In this paper, we present a technique for using the fine resolution in the high frequency channel to improve the localization of freeze/thaw boundaries. By using Gaussian convolution, or Gaussian filtering, to perform resolution compensation, it becomes possible to register boundaries observed at coarse resolution to those

observed at fine resolution. In the sections that follow, we review the Freeze Indicator work of Zuerndorfer et. al. [1989], and discuss the use of Gaussian filtering for resolution compensation and its application to freeze/thaw boundary mappings.

FREEZE INDICATOR

Freezing influences the measured radiobrightness temperature, T_b , of the ground, as observed by a satellite microwave radiometer, through parameters in the approximation [Ulaby et. al., 1981],

$$T_b = e T_0 + (1 - e) T_{sky},$$

where e and T_0 are the emissivity and surface temperature of the ground, respectively, and T_{sky} is the effective sky brightness. Atmospheric transmissivity is ignored in this approximation. Frozen ground exhibits signatures of (1) lower thermal temperatures, T_0 , (2) higher emissivity, e , and (3) a decrease in brightness temperatures with microwave frequency,

$$\frac{\partial T_b}{\partial f} < 0.$$

Signatures (1) and (2) are well understood, but are generally ambiguous indicators of frozen ground. Ambiguities arise because changes in radiobrightness that result from freezing the ground may be either positive or negative, depending upon the soil moisture content. A typical dry soil emissivity of 0.8 will yield a 8° radiobrightness decrease for a 10° decrease in thermal temperature (enough to completely freeze the ground), with relatively little change in soil emissivity. However, in moist soils, freezing causes an increase in soil emissivity, and a subsequent increase in radiobrightness.

Water molecules in frozen plants and soils are not free to align themselves with microwave electric fields. This constraint upon the rotational freedom of water gives rise to an apparent dryness of frozen plants and soils. The consequence is a decrease in the real part of the dielectric constant, ϵ' , and an increase in soil emissivity. For example, the real part of dielectric constants, ϵ' , and corresponding emissivities at nadir, $e(0)$, of two, homogeneous, smooth surfaced, 15% moist soils at 10 GHz are (ϵ' from Hoekstra and Delaney [1974]):

Material	+ 5° C			5° C		
	ϵ'	$e(0)$	T_b	ϵ'	$e(0)$	T_b
Goodrich Clay	8.2	0.77	221	4.9	0.86	235
Fairbanks Silt	9.6	0.74	214	4.1	0.89	242

Because of increasing emissivity with freezing, a 10° decrease in the clay or silt soil temperatures, from +5° C to -5° C, would cause an increase in T_b of approximately +14 K or +28 K, respectively. The positive direction of change in T_b with soil freezing will cause confusion in discrimination between soils that are frozen and cold, and soils that are warm and dry.

The shift in emissivity with freezing is most pronounced at the lower microwave frequencies. At 37 GHz, the effect is reduced, although not absent. Because the 37 GHz radiobrightness is less dependent upon soil moisture, it does exhibit a stronger correlation with air temperature than do the lower frequency radiobrightnesses. This higher correlation also occurs because air and surface temperatures tend to agree, while air and subsurface temperatures (i.e., those temperatures that influence longer wavelength radiobrightness) often differ. That is, the 37 GHz radiobrightness offers a more reliable estimate of sub-zero soil surface temperatures than do lower frequency radiobrightnesses. However, discrimination based only on 37 GHz radiobrightness would misclassify too often.

Zuerndorfer et al. [1989] suggest a third signature of frozen soil. Freezing reduces the imaginary part of the dielectric constant, ϵ'' , proportionally more than it does the real part, ϵ' . The loss tangent, $\tan \delta = \epsilon''/\epsilon'$, is a measure of the attenuation per microwave wavelength. Reduced loss tangent, or lower attenuation, means that thermally emitted photons originate deeper within emitting media. That is, the effective depth of emission, z_e , ($1-e^{-1}$ of the emission originates above z_e) becomes a larger fraction of the free-space wavelength, λ_0 [England, 1974, 1975, 1976, and 1977]. For example, Goodrich Clay and Fairbanks Silt exhibit the following increase of z_e with freezing (data from Hoekstra and Delaney [1974]):

Material	+ 5° C				-5° C			
	ϵ'	ϵ''	$\tan \delta$	z_e	ϵ'	ϵ''	$\tan \delta$	z_e
Goodrich Clay	8.2	3.5	0.43	$0.13 \lambda_0$	4.9	1.0	0.20	$0.36 \lambda_0$
Fairbanks Silt	9.6	5.0	0.52	$0.10 \lambda_0$	4.1	0.02	0.005	$15.7 \lambda_0$

The effective emission depth of moist soils is typically 10% of the free-space wavelength. Frozen soils have effective emission depths that may be 30% or more of free-space wavelengths. The effective emission depth of frozen sandy soils, like the Fairbanks Silt, can be several wavelengths. In the more transparent emitting media, such as frozen soil or dry snow, the greater average thermal photon path length has the effect of providing a greater opportunity for volume scattering of photons.

Volume scattering occurs because soils and plants appear increasingly heterogeneous at the scales of shorter microwave wavelengths. These heterogeneities scatter thermally emitted photons before they escape through the soil surface, and the scattering is increasingly severe at shorter wavelengths. This "law of darkening" means that for an isothermal volume scattering halfspace,

$$\frac{\partial T_b}{\partial T} < 0$$

[England, 1974]. Frozen terrain may also be snow covered. Because snow is exceedingly transparent and relatively heterogeneous to microwaves, snow exhibits significant of darkening [Edgerton et al., 1971]. That is, both frozen soil and snow can cause negative spectral gradients.

Neither a low 37 GHz radiobrightness nor a negative spectral gradient is solely adequate as a discriminant for classifying frozen soils at the relatively coarse resolutions of the Nimbus-7

SMMR. However, a 2-parameter, freeze signature comprised of the 37 GHz radiobrightness and the 10.7, 18, and 37 GHz spectral gradient, offers a promising initial discriminant for the classification of frozen soil. The preliminary decision boundaries that the soil is frozen are:

- (1) $T_b(37 \text{ GHz}) < 247 \text{ K}$,
- (2) 3-frequency, spectral gradients $< \frac{0.3 \text{ K}}{f(\text{GHz})}$.

BOUNDARY LOCALIZATION

In the Freeze Indicator of Zuerndorfer et al. [1989], spectral gradients were estimated using linear regressions of SMMR 37 GHz, 18 GHz, and 10.7 GHz radiobrightness measurements. The nominal resolutions of these channels are 30 Km, 60 Km, and 100 Km, respectively. Without compensating for the resolution differences between the channels, the spectral gradient estimates can be in error. For example, a non-zero gradient estimate can result from surfaces that have radiobrightnesses that are spatially variant but are constant with frequency. To avoid anomalous gradient estimates, the image data were compensated to a common resolution -- that is, the (coarse) resolution of the lowest frequency channel used in gradient estimation. (Such resolution compensated data is available with the SMMR data [NASA, 1978], and was used in the Freeze Indicator results of Zuerndorfer et al. [1989]). However, at this poorer spatial resolution, the Freeze Indicator does a relatively poor job of locating freeze/thaw boundaries. That is, the fine resolution information of the 37 GHz channel is lost.

To better use the fine resolution information of the 37 GHz channel, we note that freeze/thaw boundaries exist in images generated from only the higher resolution, 37 GHz data. However, as previously discussed, these boundaries are ambiguous because of classification errors between frozen and dry soils. We would like to identify those boundaries in 37 GHz images that correspond to the boundaries between frozen and thawed surfaces that were classified at coarse resolutions.

Our boundary identification and localization process for SMMR data requires three steps. First, the uncompensated 10.7 GHz, 18 GHz, and 37 GHz SMMR data is read and compensated to the resolution of the 10.7 GHz channel. Due to the inverse relation between spatial resolution and spatial filter bandwidth [Bracewell, 1986], resolution compensation can be achieved by spatial filtering. We use Gaussian filtering for resolution compensation of the 18 GHz and 37 GHz channels (i.e., 37 GHz and 18 GHz data are synthesized at the resolution of the 10.7 GHz channel by Gaussian filtering). The Gaussian filter bandwidths used in resolution compensation are calculated from the uncompensated resolutions of each channel. Second, resolution compensated data are used in the Freeze Indicator algorithm to classify frozen soil surfaces, and to identify freeze/thaw boundaries in images generated from compensated (coarse resolution) 37 GHz data. In our preliminary work, freeze/thaw boundaries for the 37 GHz parameter in the Freeze Indicator are located where the 37 GHz brightness crosses a threshold of 247 K, corresponding to a nominal T_b for a -5° C surface in the test area (i.e., a frozen surface). Third, freeze/thaw boundaries identified in compensated (coarse resolution) 37 GHz images are registered to boundaries observed in uncompensated (fine resolution) 37 GHz images. This is done by tracking boundary locations in 37 GHz images as the amount of resolution compensation is reduced. The resulting boundary locations that are registered in the uncompensated 37 GHz images are used as estimated locations of freeze/thaw boundaries on the surface.

In the boundary identification process, resolution compensation is achieved by Gaussian filtering. Only Gaussian filtering can guarantee that all boundaries observed in the (coarse resolution) compensated 37 GHz images can be registered to boundaries observed in the (fine resolution) uncompensated 37 GHz images. This result follows from scale-space filtering theory in computer vision [Witkin, 1983; Yuille and Poggio, 1986].

Figures 1-4 demonstrate preliminary results of our boundary identification process. Figure 1 shows the Freeze Indicator map of the test area of Zuerndorfer et. al. [1989] for SMMR data of midnight September 20, 1984. A geographical map of the test area -- North Dakota and the surrounding regions -- is included. The Freeze Indicator shows dark pixels for surfaces that are more likely frozen. Figure 2 shows the 37 GHz radiobrightness map of the same region, where the resolution has been compensated to that of the 10.7 GHz channel. Regions of darker pixels represent surface regions of lower radiobrightness. Shown as white pixels are the estimated freeze/thaw boundaries. Figure 3 shows a 37 GHz radiobrightness map of the region at a resolution corresponding to the 18 GHz channel. Figure 4 shows an uncompensated 37 GHz radiobrightness map. Figures 2-4 all show the freeze/thaw boundary.

Based upon the Freeze Indicator map of Figure 1, the dark regions in the 37 GHz radiobrightness map of Figure 2 would be classified as frozen. The localization improvement afforded by the higher resolution data is apparent in tracking the freeze/thaw boundaries from Figures 2-4 (i.e., as resolution is improved). In addition, new regions and boundaries appear as resolution improves, as in the dark islands in the northeast corner of Figure 4. These new regions are distinct from those classified at coarse resolution, and cannot be ascertained from the Freeze Indicator. Thus, classification of the new regions must be determined by other means.

CONCLUSIONS

In Zuerndorfer et. al. [1989], a multiple frequency, Freeze Indicator algorithm was developed which shows promise as a classifier of frozen soil. However, the common (coarse) resolution needed in the classification process results in a Freeze Indicator that has coarse resolution and, subsequently, poor localization of freeze/thaw boundaries. Use of scale-space theory permits the mapping of freeze/thaw boundaries from the coarse resolution of the compensated images to the finer resolution of the 37 GHz image.

A significant limitation to the improvements available in freeze/thaw boundary localization is the performance of the Freeze Indicator in correctly classifying surfaces. Work in determining frozen soil using radiometer data is in its preliminary stages. For the results presented in this paper, simple threshold crossings were used to determine freeze/thaw boundaries in the high frequency radiobrightness maps. Such criteria may not be optimal. As work on the Freeze Indicator develops, a better understanding of freeze/thaw boundaries will ensue and, subsequently, produce better criteria for determining freeze/thaw boundaries in the higher frequency, finer resolution maps.

REFERENCES

- Blanchard, B.J., and A.T.C. Chang, 1983, Estimation of soil moisture from Seasat SAR data, Water Res. Bull. 19, pp. 803-810.
- Bracewell, R. N., 1986, The Fourier Transform and Its Applications, McGraw-Hill.
- Burke, W.J., T. Schmugge, and J.F. Paris, 1979, Comparison of 2.8- and 21-cm microwave radiometer observations over soils with emission model calculations, JGR 84, pp. 287-294.
- Camillo, P.J., and T.J. Schmugge, 1984, Correlating rainfall with remotely sensed microwave radiation using physically based models, IEEE Trans. on Geosc. and Rem. Sens. GE-22, pp. 415-423.
- Edgerton, A.T., A. Stogryn, and G. Poe, 1971, Microwave Radiometric Investigations of Snowpacks, Final Rept. 1285R-4 of Contract 14-08-001-11828 between Aerojet-General Corp., El Monte, CA, and the U.S. Geological Survey.
- England, A.W., 1974, The effect upon microwave emissivity of volume scattering in snow, in ice, and in frozen soil, Proc. URSI Spec Mtg on Microwave Scattering and Emission from the Earth, Berne, Switzerland, 23-26 Sept., 1974.
- England, A.W., 1975, Thermal microwave emission from a scattering layer, JGR 80, pp. 4484-4496.
- England, A.W., 1976, Relative influence upon microwave emissivity of fine-scale stratigraphy, internal scattering, and dielectric properties, Pageoph 114, pp. 287-299.
- England, A.W., 1977, Microwave brightness spectra of layered media, Geophysics 42, pp. 514-521.
- Grody, N.C., 1988, Surface identification using satellite microwave radiometers, IEEE Transactions on Geoscience and Remote Sensing, V. 26, pp. 850-859.
- Hoekstra, P., and A. Delaney, 1974, Dielectric properties of soils at UHF and microwave frequencies, JGR 79, pp. 1699-1708.
- Moik, J., 1980, Digital Processing of Remotely Sensed Images, NASA, NASA SP-431.
- NASA, 1978, The Scanning Multichannel Microwave Radiometer (SMMR) experiment, The Nimbus-7 Users Guide, The Landsat/Nimbus Project, Goddard Space Flight Center, NASA, p. 213-245.
- Schmugge, T.J., 1983, Remote sensing of soil moisture: Recent advances, IEEE Trans. on Geosc. and Rem. Sens. GE-21, pp. 336-344.
- Schmugge, T.J., 1987, Remote sensing applications in hydrology, Rev. Geophys. 25, pp. 148-152.
- Schmugge, T.J., P.E. O'Neil, and J.R. Wang, 1986, Passive microwave soil moisture research, IEEE Trans. on Geosc. and Rem. Sens. GE-24, pp. 12-22.
- Ulaby, F.T., R.K. Moore, and A.K. Fung, 1981, Microwave Remote Sensing. Active and Passive, Addison-Wesley.
- Wang, J.R., T.J. Schmugge, W.I. Gould, W.S. Glazar, and J.E. Fuchs, 1982, A multi-frequency radiometric measurement of soil moisture content over bare and vegetated fields, Geophys. Res. Lett. 9, p. 416-419.
- Witkin, A., 1983, Scale-space filtering, Proc. Int. Joint. Conf. Artif. Intell., Karlsruhe, West Germany, p. 1019-1021.
- Yuille, A., and T. Poggio, 1986, Scaling theorems for zero crossings, IEEE Trans. Patt. Anal. Mach. Intell., Vol. PAMI-8, No. 1, p. 15-25.
- Zuerndorfer, B.W., A.E. England, M.C. Dobson, and F.T. Ulaby, 1989, Mapping freeze/thaw boundaries with SMMR data, submitted to J. Agriculture and Forest Meteorology.

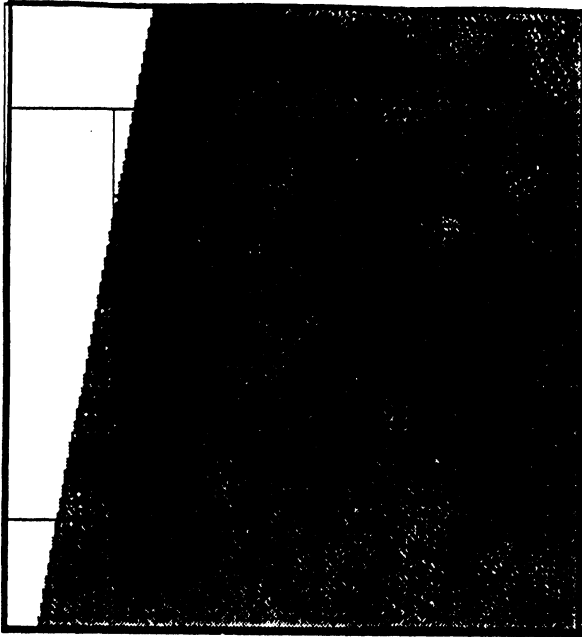


Figure 1. Freeze Indicator map of the test site, including a geographical map.

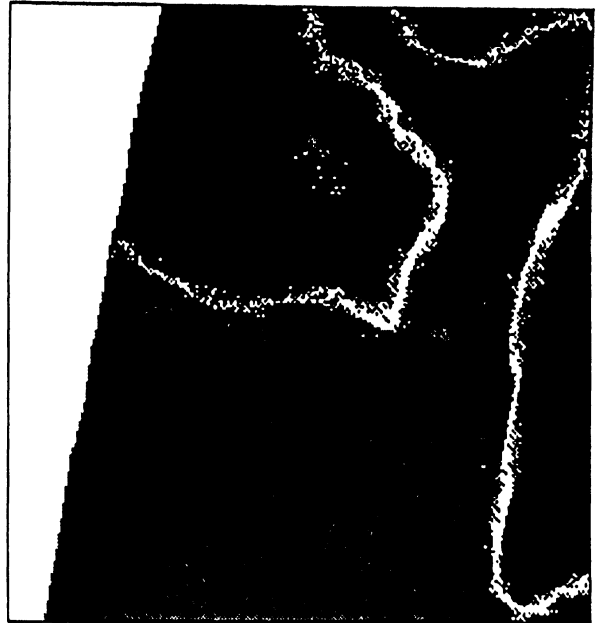


Figure 2. 37 GHz radiobrightness map of the test site at the (course) resolution of the SMMR 10.7 GHz channel.



Figure 3. 37 GHz radiobrightness map of the test site at the (medium) resolution of the SMMR 18 GHz channel.

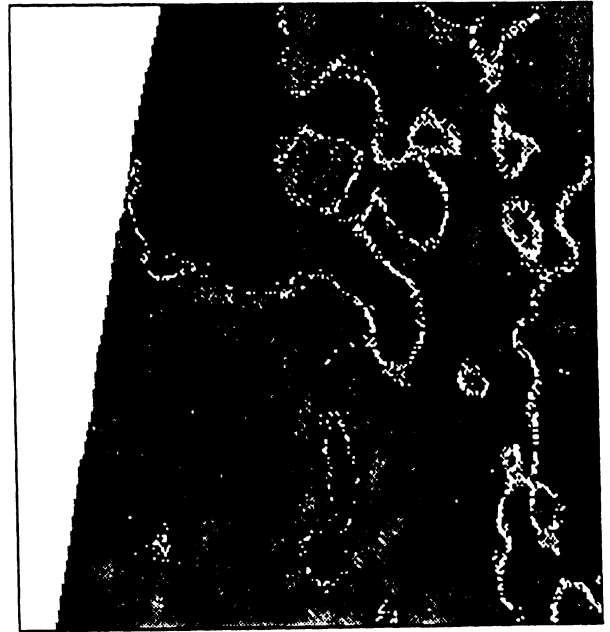


Figure 4. 37 GHz radiobrightness map of the test site at the (fine) resolution of the SMMR 37 GHz channel.